ACS Catalysis

Research Article

pubs.acs.org/acscatalysis

Selective Hydrogenation of Biomass-Based 5-Hydroxymethylfurfural over Catalyst of Palladium Immobilized on Amine-Functionalized Metal–Organic Frameworks

Jinzhu Chen,*[,†] Ruliang Liu,[†,§] Yuanyuan Guo,[†] Limin Chen,[‡] and Hui Gao[†]

[†]CAS Key Laboratory of Renewable Energy, Guangzhou Institute of Energy Conversion, Chinese Academy of Sciences, Guangzhou 510640, P.R. China

[‡]College of Environment and Energy, South China University of Technology, Guangzhou 510006, P.R. China

[§]University of Chinese Academy of Sciences, Beijing 100049, P.R. China

Supporting Information

ABSTRACT: A catalyst of palladium [Pd/MIL-101(Al)-NH_2] supported on amine-functionalized Metal–Organic Frameworks (MOFs) allows selective hydrogenation of biomass-based 5-hydroxymethylfurfural (HMF) to 2,5-dihydroxymethyl-tetrahydrofuran (DHMTHF) with 2,5-dihydroxymethylfuran (DHMF) as an observed "intermediate". The Pd/MIL-101(Al)-NH_2 was prepared by using a direct anionic exchange approach and subsequent gentle reduction. The presence of free amine moieties in the frameworks of MIL-101(Al)-NH_2 is suggested to play a key role on the formation of uniform and well-dispersed palladium nanoparticles on the support. The adsorption experiments reveal that the amine-functionalized MOF supports show preferential adsorption to hydrogenation intermediate DHMF than in the case of reactant HMF owing to an enhanced hydrophilic nature of DHMF as well as improved hydrogen bonding interactions between DHMF and the MOF support, which promotes a further hydrogenation of DHMF to DHMTHF upon the in situ formation of DHMF over Pd/MIL-101(Al)-NH_2. Moreover, our results also indicate that the observed high selectivity toward DHMTHF form HMF is closely related to the cooperation between the metallic site and the free amine moiety on the MOF support. Under the optimal conditions, a maximum DHMTHF yield of 96% with a full conversion of HMF is obtained by using Pd/MIL-101(Al)-NH_2 (Pd 3.0 wt %) catalyst at a low reaction temperature of 30 °C in aqueous medium. The research thus highlights new perspectives for aluminum-based and amine-functionalized MOF material for biomass transformation.

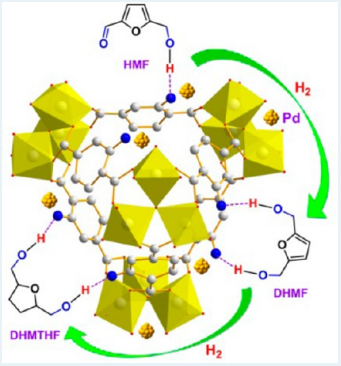

KEYWORDS: *biomass, hydrogenation, 5-hydroxymethylfurfural, palladium, metal–organic frameworks*

INTRODUCTION

Recently, the productions of fuels and chemicals from renewable biomass as an alternative to petroleum-based productions has attracted much interest, owning to diminishing fossil resources and growing concerns of environment degradation.[1−6] Currently, 5-hydroxymethylfurfural (HMF), obtained from the dehydration of sugars, is regarded as one of the most important biomass-derived platform compounds.[7,8] Recently, the hydrogenation of HMF has been investigated extensively with the conventional catalyst.[9−16] Depending on the catalyst system, the hydrogenated products can be 2,5-dihydroxymethylfuran (DHMF), 5-hydroxymethyl-2,3,4,5-tetrahydro-2-furaldehyde (HMTF), 2,5-dihydroxymethyl-tetrahydrofuran (DHMTHF), and ring-opened products such as 1,2,6-hexanetriol (1,2,6-HT), 1,2,5-hexanetriol (1,2,5-HT), and 1,2,5,6-hexanetetrol (1,2,5,6-HT). Among these hydrogenated products, DHMTHF is a typical useful chemical with wide applications as a solvent and monomer.[17,18] For example, a mixed solvent system of DHMTHF and water was recently developed as a sustainable solvent system for a tandem catalytic approach to continuous production of DHMTHF from fructose.[17] In addition, DHMTHF is an important precursor to the production of 1,6-hexanediol, which is a valuable chemical in the manufacture of polymer plastics.[11,19−24]

In the literature search for the selective hydrogenation of HMF to DHMTHF, Schiavo et al. obtained DHMTHF with high selectivities (80−100%) by using Ni-, Cu-, Pt-, Pd-, and Ru-based heterogeneous catalysts.[10] Tomishige and co-workers reported a total hydrogenation of HMF to DHMTHF with the selectivity of 96% by using Ni−Pd bimetallic catalysts.[11] It is suggested that the HMF-to-DHMTHF transformation proceeds either by the hydrogenation of aldehyde first (forming DHMF), or by the hydrogenation of ring first (yielding HMTF). Dumesic et al. studied the selective hydrogenation of HMF to DHMTHF over supported Ru, Pd, and Pt catalysts in monophasic and biphasic reactor systems.[12] The highest yields (88−91%) to DHMTHF are achieved by using Ru supported on the materials with high isoelectric points; moreover, the

Received: August 29, 2014
Revised: December 13, 2014
Published: December 16, 2014

DOI: 10.1021/cs5012926
ACS Catal. 2015, 5, 722−733

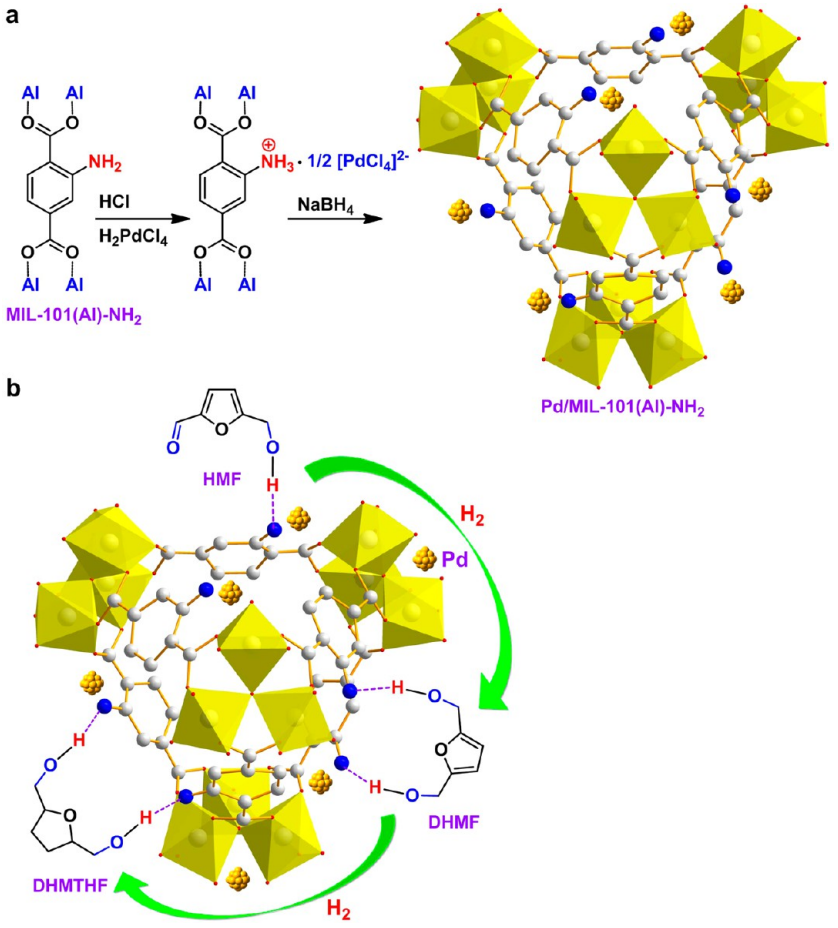

Figure 1. (a) Synthetic procedure to Pd/MIL-101(Al)-NH_2. (b) Molecular interactions in the hydrogenation of HMF over Pd/MIL-101(Al)-NH_2. Gray and blue balls represent carbon and nitrogen atoms, respectively. The aluminum octahedra is yellow in the MIL-101(Al)-NH_2. Hydrogen atoms in the MIL-101(Al)-NH_2 are omitted for clarity. The palladium nanoparticles are golden in the Pd/MIL-101(Al)-NH_2.

selectivity to DHMTHF is affected by the acidity of the aqueous solution.[12] Xu and co-workers investigated a direct conversion of fructose into DHMTHF by using a combination of acid and hydrophobic Ru/SiO_2 in a water/cyclohexane biphasic system.[13] Notably, harsh conditions such as high hydrogen pressure, high reaction temperature, high catalyst loading, and acidic reaction medium were usually required for the selective conversion of HMF to DHMTHF.[9] Therefore, the development of a greener process with the attainment of high DHMTHF selectivity under environmentally benign conditions is still a great challenge. Obviously, the development of an efficient catalyst plays a key role in this important biomass-related HMF transformation.

Recently, the biomass valorization with Metal−Organic Frameworks (MOFs) as catalysts was investigated owning to their high surface area, tunable pore sizes, controllable structures, and easy functionalization through postsynthetic modification (PSM).[25−32] For instance, the phosphotungstic acid (PTA)-encapsulated MIL-101(Cr) [PTA/MIL-101(Cr)] was reported as a solid acid catalyst for fructose dehydration to HMF.[33] The sulfonic-acid-functionalized MIL-101(Cr) [MIL-101(Cr)-SO_3H] was investigated as a solid acid for cellulose hydrolysis.[34] In addition, we recently systematically studied fructose-to-HMF transformation over sulfonic acid functionalized MOFs including MIL-101(Cr)-SO_3H, UIO-66(Zr)-SO_3H, and MIL-53(Al)-SO_3H.[35] Later, a series of amine-functionalized MOF materials were demonstrated by us as solid bases for a liquid phase transesterification of triglycerides and methanol.[36] Very recently, the acid-metal bifunctional catalyst of Ru-PTA/MIL-100(Cr) was synthesized by us to achieve a one-pot conversion of cellobiose and cellulose into sorbitol.[37]

The above developed MOF-based catalysts are, however, mainly based on PSM of known MOFs. The development of a more general and facile method to obtain a catalyst by supporting transition metal nanoparticles on MOFs remains a big challenge because of the easy agglomeration and leaching of these nanoparticles without protecting groups on the frameworks of MOF support.[38,39] Therefore, the encapsulation of highly dispersed noble metal nanoparticles such as palladium and platinum on the amine-functionalized MOFs were recently developed for the purpose of catalysis. For example, Chang and Férey reported Heck reaction by using Pd/APS-MIL-101(Cr) and Pd/ED-MIL-101(Cr) (APS and ED indicate 3-aminopropyltrialkoxysilane and ethylenediamine, respectively).[40,41] Suzuki−Miyaura cross-coupling reaction was recently investigated by the catalysts of Pd/MIL-53(Al)-NH_2,[42] Pd/UIO-66-NH_2,[43] and Pd/MIL-101(Cr)-NH_2.[44] In addition, the Pd/MIL-101(Cr)-NH_2 was further developed for the dehalogenation of aryl chlorides.[45] Yamashita and co-workers demonstrated the dehydrogenation of formic acid for hydrogen production at ambient temperature over Pd/NH_2-MIL-125.[46] The catalyst of Pt supported on PTA encapsulated in NH_2-MIL-101(Al) [Pt/PTA-NH_2-MIL-101(Al)] was recently developed for the reactions of the preferential oxidation

DOI: 10.1021/cs5012926
ACS Catal. 2015, 5, 722−733

of CO in the presence of H_2, and the hydrogenation of toluene.[47] The catalyst of Pt/UIO-66-NH_2 was reported for chemoselective hydrogenation of cinnamaldehyde.[48] The above studies thus demonstrate that amine-functionalized MOFs offer excellent possibilities for nanoparticle engineering in catalyst fabrication. Moreover, recent studies further suggested that the catalyst with nitrogen-containing support could efficiently modify its acidity/basicity, solubility/dispersibility, surface area, and especially the selectivity toward the target products in hydrogenation reactions.[49−52] Inspired by these works, an amine-functionalized MOF material MIL-101(Al)-NH_2 is targeted herein as a support to construct a bicomponent catalyst for selective hydrogenation of HMF to DHMTHF. In addition to the presence of amine functional groups on the frameworks of MIL-101(Al)-NH_2, other properties such as crystalline structure, high porosity, and high chemical/thermal stability (up to 377 °C) make MIL-101(Al)-NH_2 particularly attractive for the fabrication of hydrogenation catalyst.[53]

In this research, we report the immobilization of uniform and highly dispersed palladium nanoparticles over the MIL-101(Al)-NH_2 through the reaction pathway of anionic exchange followed by gentle reduction (Figure 1a). In addition, the resulting composite Pd/MIL-101(Al)-NH_2 shows excellent catalytic performance toward the selective hydrogenation of HMF to DHMTHF (Figure 1b). Under the optimal conditions, a maximum DHMTHF selectivity of 96% with a full conversion of HMF is obtained by using Pd/MIL-101(Al)-NH_2 catalyst at a low reaction temperature of 30 °C. The presence of free amine moieties in the frameworks of MIL-101(Al)-NH_2 is suggested to play a key role on the formation of uniform and well-dispersed palladium nanoparticles on the support (Figure 1a). Moreover, our results also indicate that the observed high selectivity toward DHMTHF form HMF is closely related to the cooperation between metallic site and free amine moiety on the MOF support (Figure 1b).

EXPERIMENTAL SECTION

Materials. Unless otherwise stated, all chemicals in this work were commercially available and used without further purification. Terephthalic acid, 2-aminoterephthalic acid, 5-hydroxymethylfurfural (HMF), sodium hydroxide, hydrochloric acid (36−38 wt % aqueous solution), aluminum chloride hexahydrate ($AlCl_3·6H_2O$), aluminum nitrate nonahydrate [$Al(NO_3)_3·9H_2O$], and chromium nitrate nonahydrate [$Cr(NO_3)_3·9H_2O$] were purchased from Aladdin Industrial Inc. (Shanghai, P. R. China). *N*,*N*-dimethylformamide (DMF), methanol, sodium borohydride ($NaBH_4$), and acetone were purchased from Sinopharm Chemical Reagent Co. Ltd. (Shanghai, P. R. China). Palladium chloride ($PdCl_2$) was provided by Kunming Boren Precious Metals Co. Ltd. (Kunming, P. R. China). Hydrogen gas (>99.999%) was obtained from Huate Co. Ltd. (Foshan, P. R. China). Deionized pure water from Millipore-Milli Q Plus System was used as solvent.

Characterization. The Brunauer−Emmett−Teller (BET) surface area measurements were performed with N_2 adsorption−desorption isotherms at 77 K (SI-MP-10/PoreMaster 33, Quantachrome). After degassed under vacuum at 393 K for 24 h and then measured over the range of $10^{-6} < P/P_0 < 0.1$. The specific surface areas were evaluated using the BET method in the P/P_0 range 0.05 to 0.3. The powder X-ray diffraction (XRD) patterns of the MOF samples were obtained by a Bruker Advance D8 diffractometer at 40 kV and 40 mA, using Ni-filtered Cu Kα radiation with a scan speed of 0.3 s/step, a step size of 0.02° in 2θ, and a 2θ range of 5−50. Approximately 15 mg of sample was dehydrated under high vacuum at 100 °C overnight before XRD analysis. The X-ray photoelectron spectroscopy (XPS) spectra analysis was performed with a Kratos Axis Ultra (DLD) photoelectron spectrometer operated at 15 kV and 10 mA at a pressure of about 5×10^{-9} Torr using AlKa as the excitation source (1486.6 eV). C 1s photoelectron peak (BE = 284.2 eV) was used for the binding energy calibration. The palladium contents in the catalysts Pd/MOFs were quantitatively determined by inductively coupled plasma-atomic emission spectroscopy (ICP-AES) analysis on the PerkinElmer Optima 8000 instrument. The samples were digested in the sodium hydroxide and then aqua regia was added to the mixture to digest the noble metal. The morphological analysis of the catalyst was carried out using transmission electron microscopy (TEM, JEM-2010HR). Samples for TEM studies were prepared by placing a drop of the suspension of Pd/MOFs sample in ethanol onto a carbon-coated copper grid, followed by evaporating the solvent. High-performance liquid chromatography−mass spectrometry (HPLC-MS) analysis was performed by using an Agilent HPLC-MS instrument equipped with a Column Comp. G1316C (column temperature: 40 °C) and MS Q-TOF G6540B (ion source: dual ESI). The ^{1}H NMR and $^{13}C\{^1H\}$ NMR spectra of DHMF and DHMTHF were recorded on Bruker AV III 400 at 25 °C with DMSO-d_6 as solvent.

Catalyst Preparation. MIL-101(Al)-NH_2,[53] MIL-53(Al)-NH_2,[54,55] MIL-53(Al),[56] and MIL-101(Cr)[40,41,57] were prepared according to the literature methods.

Pd/MIL-101(Al)-NH_2. The activated MIL-101(Al)-NH_2 (500 mg) in H_2O (40 mL) was treated with hydrochloric acid to tune the pH around 4. A solution of H_2PdCl_4 [containing ca. 3.0 wt % of Pd relative to MIL-101(Al)-NH_2] was added to the above acidulated slurry under vigorous agitation for 10 min. The mixture was then stirred for another 8 h. The solid was filtered and washed with deionized water. The resulting gray sample $[MIL\text{-}101(Al)\text{-}NH_3^+]_2[PdCl_4]^{2-}$ was then reduced by sodium borohydride ($NaBH_4$, 40 mg) at 0 °C for 2 h to yield Pd/MIL-101(Al)-NH_2 (Figure 1a). The Pd/MIL-101(Al)-NH_2 (Pd 3.0 wt % based on ICP-AES) was further dried under vacuum overnight at 120 °C before use.

Pd/MIL-53(Al)-NH_2. Pd/MIL-53(Al)-NH_2 (Pd 3.0 wt % based on ICP-AES) was prepared following the same synthetic procedure as for Pd/MIL-101(Al)-NH_2 used except that MIL-101(Al)-NH_2 was replaced by MIL-53(Al)-NH_2.

Pd/MIL-53(Al) and Pd/MIL-101(Cr). An aqueous solution of H_2PdCl_4 (containing ca. 3.0 wt % Pd) was added to the activated MOFs [500 mg, MIL-53(Al) or MIL-101(Cr)], which was suspended in water (40 mL) under vigorous agitation for 10 min. The mixture was then stirred for another 24 h. The solid was centrifuged and washed with deionized water and ethanol, respectively. The resulting MOF samples containing palladium salts were then reduced by sodium borohydride ($NaBH_4$, 40 mg) at 0 °C for 2 h to obtain Pd/MIL-53(Al) (Pd 1.7 wt % based on ICP-AES) or Pd/MIL-101(Cr) (Pd 1.4 wt % based on ICP-AES).

Catalytic Performance. The selective hydrogenation of HMF was carried out in a 60 mL stainless steel reactor equipped with a magnetic stirrer. In a typical run, HMF (126 mg, 1.0 mmol), Pd/MIL-101(Al)-NH_2 (20 mg) were added to water (8.0 mL) in the stainless steel reactor. After purging the reactor three times with hydrogen, the outlet valve was then

DOI: 10.1021/cs5012926
ACS Catal. 2015, 5, 722−733

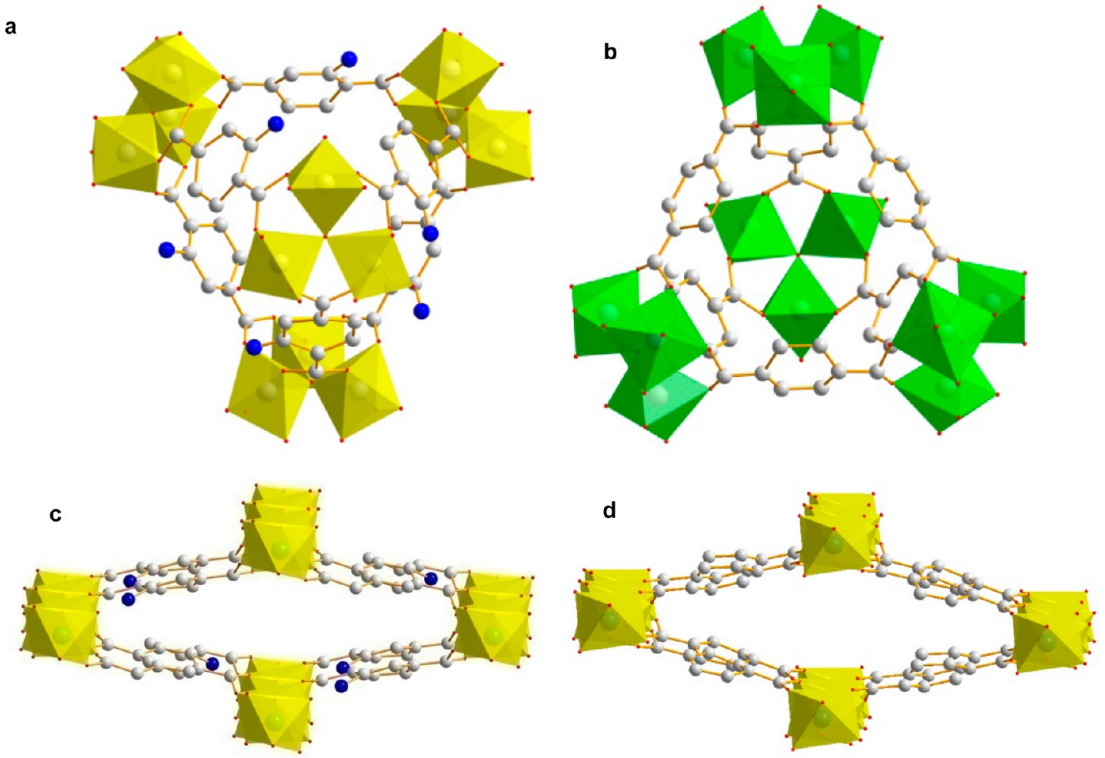

Figure 2. Structures of (a) MIL-101(Al)-NH_2, (b) MIL-101(Cr), (c) MIL-53(Al)-NH_2, and (d) MIL-53(Al). Gray and blue balls represent carbon and nitrogen atoms, respectively. The aluminum octahedra is yellow in the MIL-101(Al)-NH_2, MIL-53(Al)-NH_2, and MIL-53(Al). The chromium octahedra is green in the MIL-101(Cr). Hydrogen atoms are omitted for clarity.

closed to maintain 1.0 MPa of hydrogen pressure (ambient temperature). The reaction was conducted at 30 °C for 12 h with a stirring speed of 600 rpm. After the reaction was halted, the reactor was cooled to room temperature. The mixture was filtered, decanted into a volumetric flask using water as diluent, and then analyzed by high-performance liquid chromatography (HPLC) and high-performance liquid chromatography–mass spectrometer (HPLC-MS). The analysis of products was conducted on HPLC (Shimadu LC-20AT) with a Shodex Sugar SH-1011 column (300 × 8 mm) using HPLC grade H_2SO_4 (0.005 M) water solution as the eluent at a column temperature of 50 °C and a flow rate of 0.5 mL min^{-1}. The conversion of HMF was determined by a UV detector (320 nm); whereas, the concentrations of products such as DHMF, and DHMTHF were monitored by a refractive index (RI) indicator. DHMF: ^{1}H NMR (400 MHz, DMSO-d_6) δ 6.18 (s, 1H), 5.17 (t, J = 5.6 Hz, 1H), 4.35 (d, J = 5.4 Hz, 2H). $^{13}C\{^1H\}$ NMR (101 MHz, DMSO-d_6) δ 154.7, 107.4, 55.8. Mass spectrum (EI) m/z 128.1 (M^+). DHMTHF: ^{1}H NMR (400 MHz, DMSO-d_6) δ 4.56 (d, J = 5.1 Hz, 1H), 3.90–3.73 (m, 1H), 3.34 (t, J = 4.6 Hz, 2H), 1.85–1.52 (m, 2H). $^{13}C\{^1H\}$ NMR (101 MHz, DMSO-d_6) δ 79.8, 64.0, 27.3. Mass spectrum (EI) m/z 133.1 (MH^+).

Adsorption Experiments. All of the investigated MOFs were dried at 80 °C under high vacuum for 24 h before adsorption experiments. Adsorption of HMF over various MOFs was investigated by addition of activated MOFs (100 mg) to the solutions of HMF (0.6 mmol) in water (25 mL). The mixture was stirred at 25 °C for 4.0 h. The amount of adsorbed HMF over MOFs was determined chromatographically (HPLC) by the corresponding concentration change of HMF in water. The adsorption of DHMF over various MOFs was performed with the same procedure to that of HMF except that HMF was replaced by DHMF.

RESULTS AND DISCUSSION

Preparation and Characterization of Pd/MOF Catalysts. In this research, both amine-functionalized MOFs [MIL-101(Al)-NH_2 and MIL-53(Al)-NH_2] and MOF materials without amine functional groups on the frameworks [MIL-53(Al) and MIL-101(Cr)] were introduced to Pd catalyst as the supports. The influence of the MOF support on the catalytic performance of Pd catalysts for the HMF hydrogenation and especially the selectivity toward DHMTHF was investigated. For the comparison of MIL-101(Al)-NH_2 (Figure 2a) and MIL-53(Al)-NH_2 (Figure 2c), both of them are aluminum-based MOF materials and contain amine functional groups on the frameworks with, however, different structures. According to the literature, the MIL-101(Al)-NH_2 possesses two different types of quasispherical mesoporous cages formed by 12 pentagonal and 16 faces, respectively.[53] However, the MIL-53(Al)-NH_2 is built up from infinite chains of corner-sharing $AlO_4(OH)_2$ octahedra interconnected by dicarboxylate groups.[55] In the cases of MIL-53(Al)-NH_2 (Figure 2c) and MIL-53(Al) (Figure 2d), both of them share a similar structure; however, MIL-53(Al)-NH_2 contains amine functional groups on the frameworks as a result of the different connecting organic linker of 2-aminoterephthalic acid for MIL-53(Al)-NH_2 and terephthalic acid for MIL-53(Al), respectively.[55,56] As the MIL-101 series, both MIL-101(Al)-NH_2 (Figure 2a) and MIL-101(Cr) (Figure 2b) share a same topology of the framework. However, the connecting organic linker of 2-aminoterephthalic acid in the MIL-101(Al)-NH_2 is replaced by terephthalic acid in the MIL-101(Cr), and the metal site of aluminum in MIL-

DOI: 10.1021/cs5012926
ACS Catal. 2015, 5, 722–733

101(Al)-NH_2 is replaced by chromium in MIL-101-(Cr).[40,41,53,57] Therefore, the structure of MIL-101(Al)-NH_2 is similar to that of MIL-101(Cr) but possesses the amine groups on the frameworks.

As shown in Figure 1a, the synthetic procedure of Pd/MIL-101(Al)-NH_2 consists of the neutralization of the amine groups on the MIL-101(Al)-NH_2 with an aqueous HCl solution, anionic exchange reactions between the chloride anions of [MIL-101(Al)-NH_3^+]Cl^- and anionic $[PdCl_4]^{2-}$ of H_2PdCl_4, and finally the gentle reduction of palladium metal of [MIL-101(Al)-NH_3^+]$_2[PdCl_4]^{2-}$ with $NaBH_4$ at low reaction temperature (Figure 1a). Pd/MIL-53(Al)-NH_2 was prepared following the same synthetic procedure as for Pd/MIL-101(Al)-NH_2 used except that MIL-101(Al)-NH_2 was replaced by MIL-53(Al)-NH_2. In the cases of Pd/MIL-53(Al) and Pd/MIL-101(Cr), a conventional incipient wetness impregnation was involved for their preparation with the corresponding supports.

The specific surface areas of the Pd/MOF catalyst samples were measured by N_2 adsorption/desorption at 77 K, and the results are presented in Table 1. Compared with the bare MIL-101(Al)-NH_2, the resulting pore modification is visible on the N_2 adsorption/desorption isotherms after the Pd loading (Figure 3). As expected, the Pd/MIL-101(Al)-NH_2 exhibits a significant decrease of porous surface area with the increase of palladium loading levels. After the loading of palladium nanoparticles, the Brunauer–Emmett–Teller (BET) surface area of MIL-101(Al)-NH_2 (1025.8 m^2 g^{-1}) significantly decreases to 871.9 m^2 g^{-1} for Pd content of 0.9 wt %, and to 529.2 m^2 g^{-1} for Pd content of 4.4 wt % (Table 1). The appreciable decreases in nitrogen adsorption amount and surface area indicate that the cavities of MIL-101(Al)-NH_2 are presumably occupied by highly dispersed Pd nanoparticles or Pd nanoparticles deposited on the pore surface of MIL-101(Al)-NH_2.[58] The similar results were also observed on other Pd/MOF catalysts, the BET surface area of Pd/MOF significantly decreased when compared with its corresponding bare MOF support (Table 1 and Figure S1 Supporting Information).

Table 1. Textural Properties of Various MOF Support and Pd/MOF Catalysts

samples	surface area[a] [m^2 g^{-1}]	pore volume[b] [cm^3 g^{-1}]
MIL-101(Al)-NH_2	1025.8	1.36
Pd/MIL-101(Al)-NH_2 (Pd 0.9 wt %)	871.9	0.96
Pd/MIL-101(Al)-NH_2 (Pd 3.0 wt %)	615.7	0.69
Pd/MIL-101(Al)-NH_2 (Pd 2.8 wt %)[c]	542.8	0.55
Pd/MIL-101(Al)-NH_2 (Pd 4.4 wt %)	529.2	0.51
MIL-53(Al)	1494.2	1.81
Pd/MIL-53(Al) (Pd 1.7 wt %)	1046.5	1.09
MIL-53(Al)-NH_2	217.6	1.75
Pd/MIL-53(Al)-NH_2 (Pd 3.0 wt %)	87.4	0.38
MIL-101(Cr)	1517.0	1.86
Pd/MIL-101(Cr) (Pd 1.4 wt %)	864.8	0.71

[a]Langmuir surface area was evaluated using the Brunauer–Emmett–Teller (BET) method in the p/p_0 range of 0.05 to 0.3. [b]Pore size distribution curves were calculated using the adsorption branch of the isotherms and the Barrett–Joyner–Halenda (BJH) method, and pore sizes were obtained from the peak positions of the distribution curves. [c]Recovered Pd/MIL-101(Al)-NH_2 with the reaction conditions described in Figure 11b.

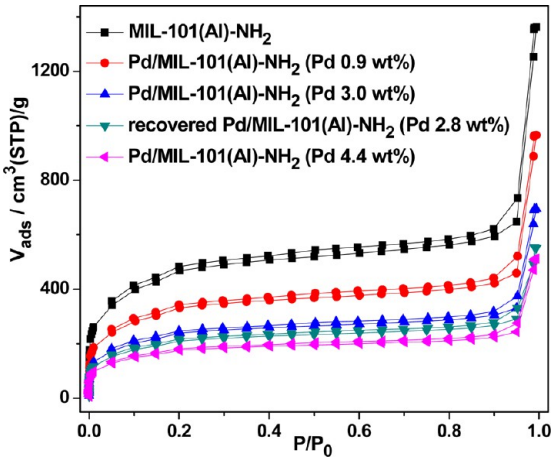

Figure 3. N_2 adsorption–desorption isotherms of MIL-101(Al)-NH_2, Pd/MIL-101(Al)-NH_2 with different Pd loading levels (Pd 0.9–4.4 wt %), and recovered Pd/MIL-101(Al)-NH_2 (Pd 2.8 wt %) with the reaction conditions described in Figure 11b.

To identify the active species for the hydrogenation, MIL-101(Al)-NH_2 and Pd/MIL-101(Al)-NH_2 were further compared by powder X-ray powder diffraction (XRD). The powder XRD pattern of MIL-101(Al)-NH_2 matches well with the published results (Figure 4a).[53] After the immobilization of Pd nanoparticles, the structure of MIL-101(Al)-NH_2 is mostly preserved regardless of the increased Pd content in the material Pd/MIL-101(Al)-NH_2 (Figure 4a). However, some variations of the Bragg intensities were observed, indicating the successful loading of Pd nanoparticles in the MIL-101(Al)-NH_2. In addition, no diffraction peaks corresponding to Pd crystallite can be observed over the Pd/MIL-101(Al)-NH_2, which implies that the highly dispersed Pd species exist in the very small nanoparticles or in amorphous structure. Moreover, Figure 4b shows the XRD patterns of other Pd/MOF catalysts and the corresponding MOF supports, and similar results were also observed.

As indicated in the transmission electron microscopy (TEM) images, the Pd nanoparticles were highly dispersed on MIL-101(Al)-NH_2 with a uniform size (Figure 5a–f). Notably, the TEM image of Pd/MIL-101(Al)-NH_2 (Pd 0.9 wt %) shows that the Pd nanoparticles are embedded inside the crystals and are homogeneously distributed throughout the crystals of MIL-101(Al)-NH_2 (Figure 5a), further indicating the encapsulation of Pd nanoparticles within the interior of MIL-101(Al)-NH_2. Moreover, the average nanoparticle size of Pd in Pd/MIL-101(Al)-NH_2 only slightly increased with the Pd loading levels from 2.8 nm for Pd content of 0.9 wt % to 3.1 nm for Pd content of 4.4 wt % (Figure 5a–f). In the case of Pd/MIL-53(Al)-NH_2, again, well dispersed and uniform Pd nanoparticles were observed throughout MIL-53(Al)-NH_2 support with an average nanoparticle size of 2.4 nm (Figure 5i, j). In sharp contrast to the MOF support without amine group on the frameworks, the Pd nanoparticles were readily accumulated over the MIL-53(Al) with a mean nanoparticle size of 4.0 nm for 1.7 wt % loading level of Pd in the Pd/MIL-53(Al) (Figure 5k, l), further indicating an efficient stabilization effect of the MIL-101(Al)-NH_2 and MIL-53(Al)-NH_2 supports on the palladium nanoparticles. For Pd/MIL-101(Cr) (Pd 1.4 wt %), the size of the Pd nanoparticles was around 3.7 nm (Figure 5m, n). Moreover, these larger Pd nanoparticles were found

DOI: 10.1021/cs5012926
ACS Catal. 2015, 5, 722–733

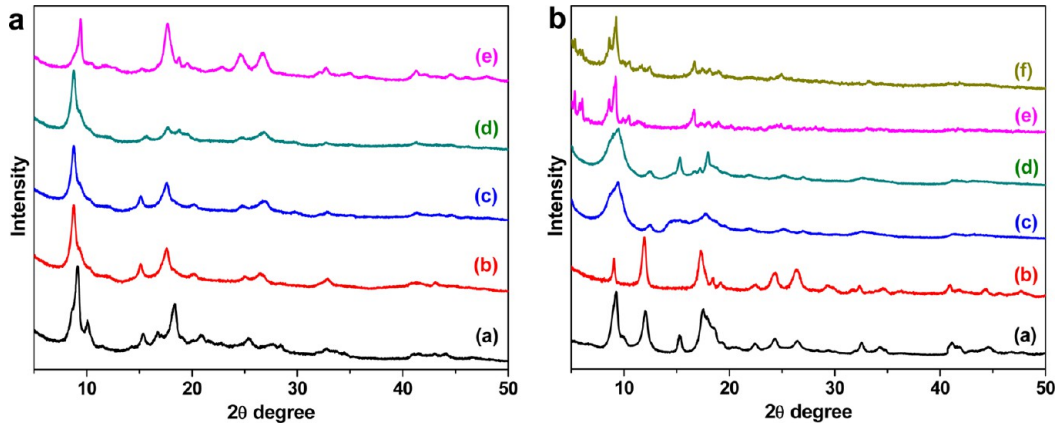

Figure 4. (Panel a) XRD patterns of (a) MIL-101(Al)-NH_2, (b) Pd/MIL-101(Al)-NH_2 (Pd 0.9 wt %), (c) Pd/MIL-101(Al)-NH_2 (Pd 3.0 wt %), (d) Pd/MIL-101(Al)-NH_2 (Pd 4.4 wt %), (e) recovered Pd/MIL-101(Al)-NH_2 (Pd 2.8 wt %) with the reaction conditions described in Figure 11b. (Panel b) XRD patterns of (a) MIL-53(Al)-NH_2, (b) Pd/MIL-53(Al)-NH_2 (Pd 3.0 wt %), (c) MIL-53(Al), (d) Pd/MIL-53(Al) (Pd 1.7 wt %), (e) MIL-101(Cr), (f) Pd/MIL-101(Cr) (Pd 1.4 wt %).

accumulated mainly on the surfaces of the MIL-101(Cr) crystals, as shown by the TEM (Figure 5m).

The X-ray photoelectron spectroscopy (XPS) survey spectra of the Pd/MIL-101(Al)-NH_2 sample is shown in Figure 6a. The photoelectron peaks of main elements on the surface of Pd/MIL-101(Al)-NH_2 appear at the binding energies of 74.4 eV (Al 2P), 281.8 eV (C 1s), 335.6 eV (Pd 3d), 399.2 eV (N 1s), and 530.4 eV (O 1s), respectively, further confirming the presence of amine group on the framework of MIL-101(Al)-NH_2 and palladium nanoparticles over MIL-101(Al)-NH_2. The Pd 3d XPS spectrum of Pd/MIL-101(Al)-NH_2 shows two main peaks appeared at 340.9 and 335.6 eV correspond to Pd 3d3/2 and Pd 3d5/2, respectively (Figure 6b), indicating that the Pd(II) cations in the $[\text{MIL-101(Al)-NH}_3^+]_2[PdCl_4]^{2-}$ were successfully reduced to Pd(0) in the Pd/MIL-101(Al)-NH_2 after the reduction by sodium borohydride.[42]

HMF Hydrogenation over Pd/MOF Catalysts. The prepared Pd/MOF catalysts were investigated for selective hydrogenation of HMF. Hydrogenation of HMF leads to the formation of DHMF, a further hydrogenation of DHMF results in the transformation of DHMF to DHMTHF (Figure 1b). In addition to DHMF and DHMTHF, other polyols such as hexanetriol (HT) were observed by HPLC as byproducts during the process of HMF hydrogenation.[12,59] In this research, we performed the hydrogenation of HMF under pressurized hydrogen conditions in water using Pd/MOF as the catalyst. An initial experiment was carried out to investigate the effect of the reaction temperature and Pd loading levels in the Pd/MIL-101(Al)-NH_2 catalyst on the HMF hydrogenation. The HMF hydrogenation was performed over Pd/MIL-101(Al)-NH_2 with the Pd content ranging from 0.9 wt % to 4.4 wt % at the reaction temperature from 30 to 100 °C (Figure 7). Generally, a full conversion of HMF was observed under all investigated condition, suggesting an efficient hydrogenation activity of Pd/MIL-101(Al)-NH_2 toward HMF. The selectivity of DHMTHF increased with reaction temperature ranging from 40 to 80 °C at all Pd loading levels of the catalysts. The selectivity of DHMF decreased with the reaction temperature from 40 to 80 °C under the above conditions, suggesting that increasing the reaction temperature promotes a further hydrogenation of DHMF to DHMTHF (Figure 7). In the case of the hydrogenation performed at 100 °C, a full conversion of DHMF and a significantly increased selectivity to HT were observed over the Pd/MIL-101(Al)-NH_2 with various Pd loading levels, suggesting that raising the reaction temperature promotes the DHMF hydrogenation as well as the HT formation.

The influence of the Pd loading levels on the HMF hydrogenation indicated that the transformation rates both for DHMF-to-DHMTHF and DHMF-to-HT increased with the Pd content in the catalyst under the specified reaction temperature (Figure 7). Moreover, the selectivity of HT increased from 6% to 12% at 100 °C with the increasing Pd loading level from 0.9 wt % to 4.4 wt %, indicating that the increasing Pd content in the catalyst leads to an increased selectivity to HT. Obviously, low reaction temperature, prolonged reaction time and moderate loading level of Pd in the catalyst favor a high selectivity to DHMTHF. Under the optimal conditions, a maximum DHMTHF selectivity of 96% with full conversions of both HMF and DHMF were obtained by using the Pd/MIL-101(Al)-NH_2 (Pd 3.0 wt %) at an optimal reaction temperature of 30 °C and reaction time of 12 h (Figure 7).

The influence of H_2 pressure on the reaction revealed that the increase in H_2 pressure from 0.5 to 1.0 MPa significantly increased the hydrogenation rates both for HMF-to-DHMF and the subsequent DHMF-to-DHMTHF transformations (Figure 8). HMF achieved a full conversion at 1.0 MPa; meanwhile, DHMTHF reached a maximum selectivity of 86% under the investigated conditions. DHMF was observed to be formed with a maximum selectivity of 67% at 0.5 MPa and later consumed with the increased H_2 pressure. The selectivity of HT significantly increased from 3% at a H_2 pressure of 0.5 MPa to 26% at the H_2 pressure of 3.0 MPa, suggesting that increasing the H_2 pressure promotes hydrolytic hydrogenation of DHMF as well as hydrogenolysis of DHMTHF to give HT.

Figure 9 shows a typical reaction profile for the hydrogenation of HMF over Pd/MIL-101(Al)-NH_2 at low reaction temperature of 30 °C in aqueous media. HMF was quickly converted into DHMF and DHMTHF with the selectivities of 67% and 32%, respectively, at 1.0 h. After this time, the selectivity of DHMF quickly declined with the increased selectivity of DHMTHF, owing to a further hydrogenation of DHMF. HMF was completely converted into DHMF and DHMTHF at the reaction time of 5.0 h with, however, the primary product of DHMTHF rather than DHMF. The

DOI: 10.1021/cs5012926
ACS Catal. 2015, 5, 722−733

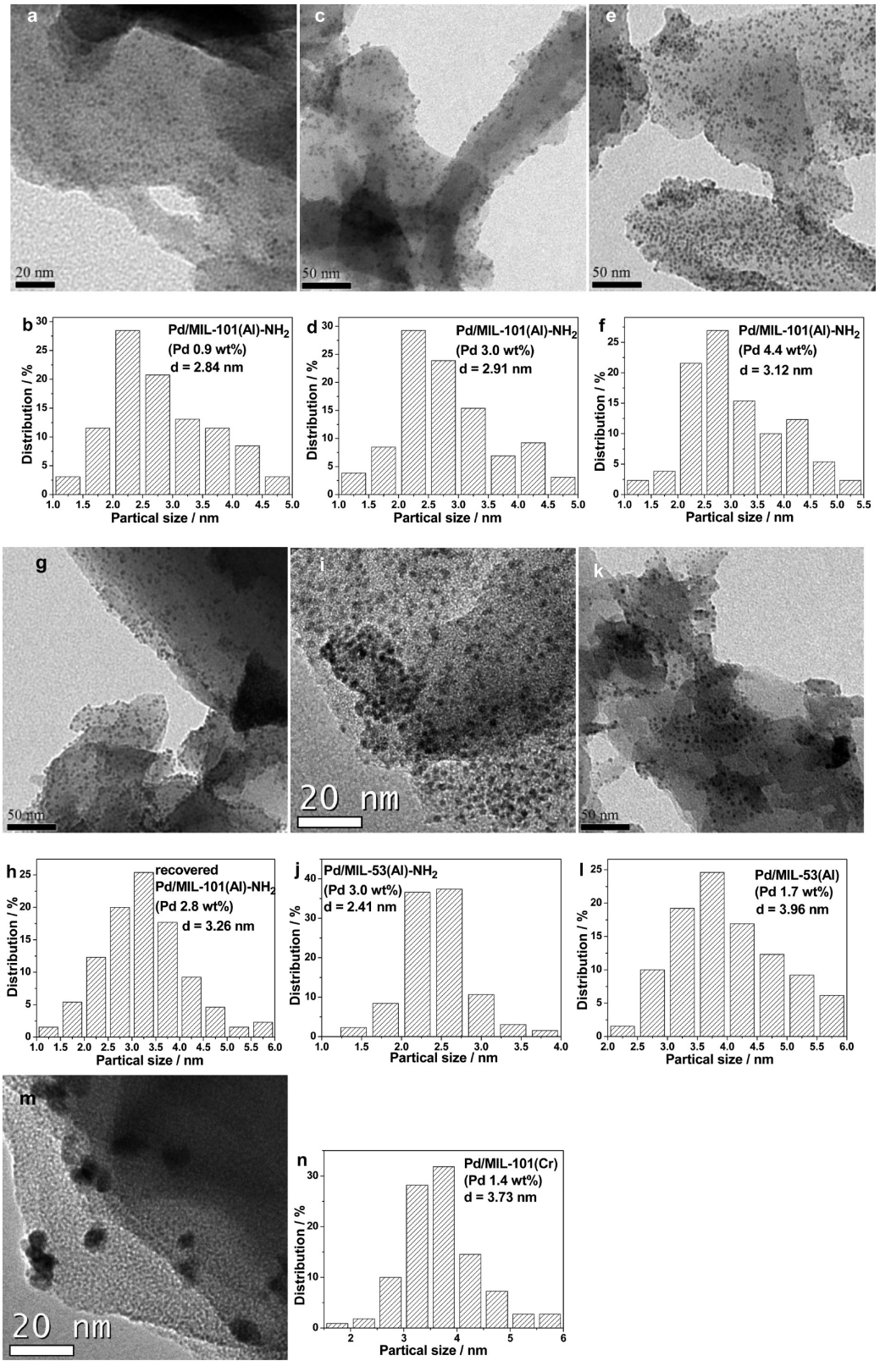

Figure 5. TEM images and particle-size distribution of (a, b) Pd/MIL-101(Al)-NH_2 (Pd 0.9 wt %), (c, d) Pd/MIL-101(Al)-NH_2 (Pd 3.0 wt %), (e, f) Pd/MIL-101(Al)-NH_2 (Pd 4.4 wt %), (g, h) recovered Pd/MIL-101(Al)-NH_2 (Pd 2.8 wt %), (i, j) Pd/MIL-53(Al)-NH_2 (Pd 3.0 wt %), (k, l) Pd/MIL-53(Al) (Pd 1.7 wt %), (m, n) Pd/MIL-101(Cr) (Pd 1.4 wt %).

selectivity of DHMTHF reaches a maximum of 96% at the reaction time of 12.0 h with a full conversion of DHMF. HT was observed as byproduct with the selectivities ranging from trace to 4%. The above reaction profile further suggested that the hydrogenation of HMF was stepwise with DHMF as the observed "intermediate" (Figure 1b).

Effect of MOF Support. Figure 10 shows the influence of the MOF support on the catalytic performance of Pd catalyst

DOI: 10.1021/cs5012926
ACS Catal. 2015, 5, 722−733

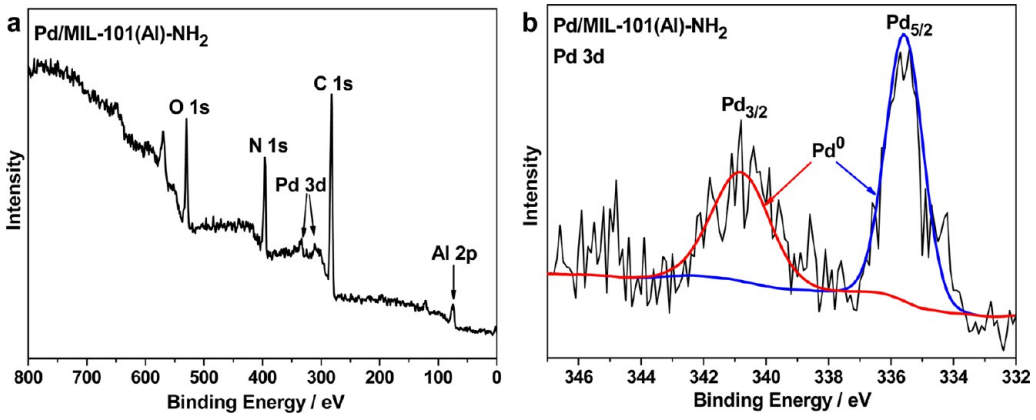

Figure 6. XPS spectra of Pd/MIL-101(Al)-NH_2 (Pd 3.0 wt %) (a) survey spectra and (b) Pd 3d.

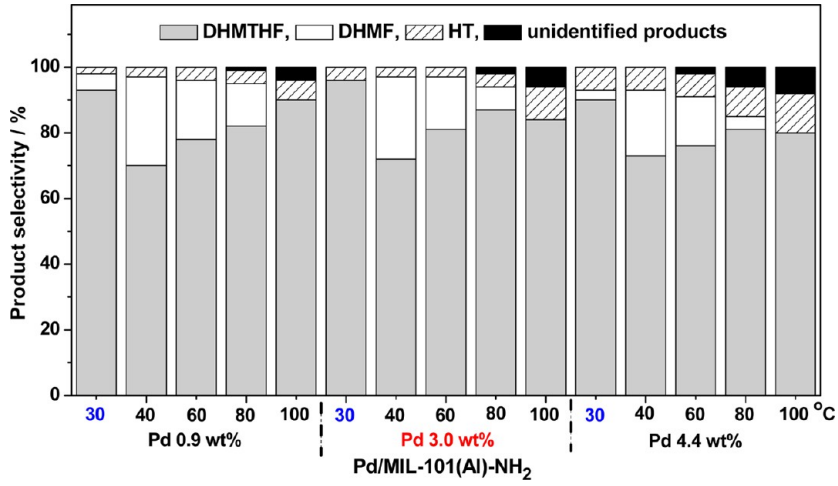

Figure 7. Influences of the reaction temperature and Pd loading levels in the catalyst Pd/MIL-101(Al)-NH_2 on the HMF hydrogenation. Reaction conditions: HMF (126 mg, 1.0 mmol), Pd/MIL-101(Al)-NH_2 (20 mg, Pd 0.9–4.4 wt %), water (8 mL), H_2 (1.0 MPa), reaction temperature and time (30 °C for 12 h and 40–100 °C for 4 h).

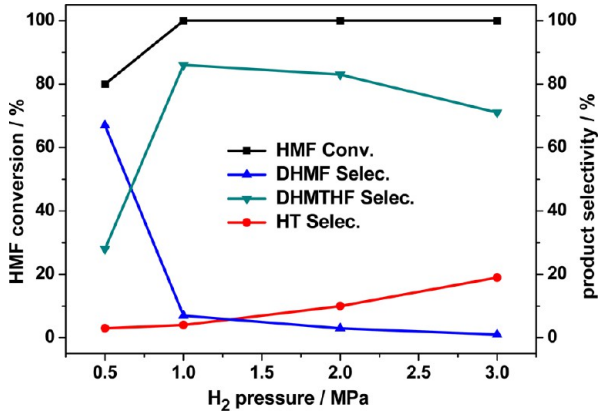

Figure 8. Effect of H_2 pressure on the HMF hydrogenation over Pd/MIL-101(Al)-NH_2. Reaction conditions: HMF (126 mg, 1.0 mmol), Pd/MIL-101(Al)-NH_2 (20 mg, Pd 3.0 wt %), water (8 mL), reaction temperature (100 °C), reaction time (2 h).

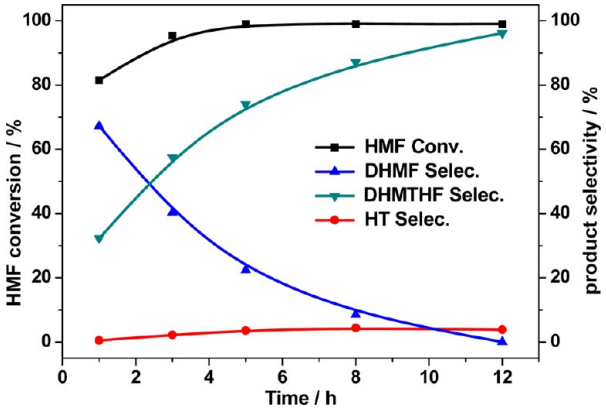

Figure 9. Selectivity to DHMF, DHMTHF, and HT as a function of reaction time for the hydrogenation of HMF over Pd/MIL-101(Al)-NH_2. Reaction condition: HMF (126 mg, 1.0 mmol), Pd/MIL-101(Al)-NH_2 (20 mg, Pd 3.0 wt %), water (8 mL), reaction temperature (30 °C), H_2 (1.0 MPa).

for the HMF hydrogenation. A full conversion of HMF was generally observed under all investigated conditions. Pd/MIL-101(Al)-NH_2 catalysts with the Pd contents of 0.9 and 3.0 wt % afforded DHMTHF selectivities of 93% and 96%, respectively, at 30 °C after 12 h. In addition to Pd/MIL-101(Al)-NH_2, Pd/MIL-53(Al)-NH_2 (Pd 3.0 wt %) also showed good catalytic performance toward HMF hydrogenation, yielding DHMTHF and DHMF selectivities of 88% and 8%, respectively, with a full conversion of HMF. In sharp contrast, the DHMTHF selectivities of 61% and 76% were observed over Pd/MIL-53(Al) (Pd 1.7 wt %) and Pd/MIL-101(Cr) (Pd 1.4 wt %),

DOI: 10.1021/cs5012926
ACS Catal. 2015, 5, 722–733

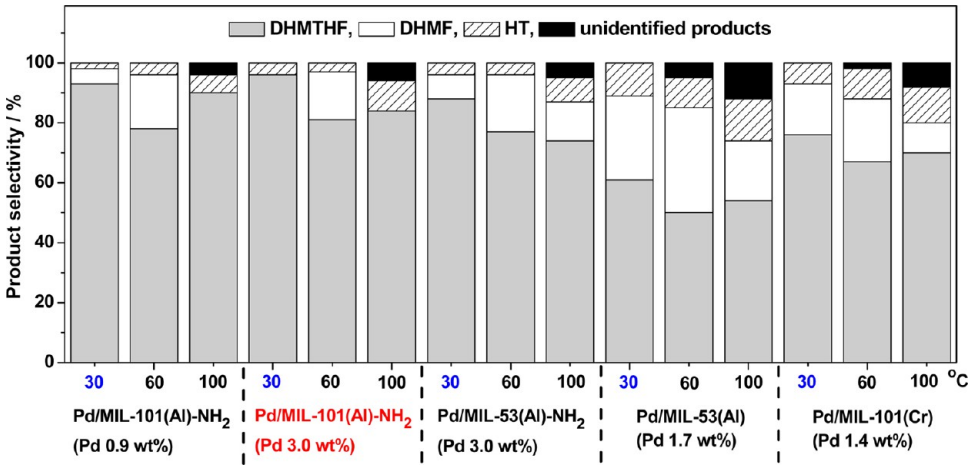

Figure 10. Effect of MOF support on the selective hydrogenation of HMF. Reaction conditions: HMF (126 mg, 1.0 mmol), catalyst [20 mg, Pd/MIL-101(Al)-NH_2, Pd/MIL-53(Al)-NH_2, Pd/MIL-53(Al) or Pd/MIL-101(Cr)], water (8 mL), reaction temperature and time (30 °C for 12 h, and 60−100 °C for 4 h).

respectively, under the investigated conditions. Therefore, Pd/MIL-101(Al)-NH_2 is considerably more active and selective to afford DHMTHF than Pd/MIL-53(Al)-NH_2, Pd/MIL-53(Al) and Pd/MIL-101(Cr) under all specified conditions. In addition, Pd/MIL-101(Al)-NH_2 shows higher catalytic performance than Pd/MIL-53(Al)-NH_2, whereas Pd/MIL-101(Cr) is more efficient to afford DHMTHF when compared with Pd/MIL-53(Al). These results can presumably be attributed to an inherent drawback of MIL-53 series on the strong adsorption and diffusion limitations in their 1-D pore structure (Figure 2c,d) when compared with a quasispherical mesoporous cage system of MIL-101 series (Figure 2a,b).[60] In addition, MIL-53 series generally possess relatively smaller surface area in comparison to the corresponding MIL-101 series (Table 1). Notably, as described in Figure 10, the influence of MOF support indicates that the Pd catalysts immobilized over amine-functionalized MOFs [Pd/MIL-101(Al)-NH_2 and Pd/MIL-53(Al)-NH_2] generally show higher selectivity to DHMTHF when compared with their analogues without amine groups on the MOF frameworks [Pd/MIL-101(Cr) and Pd/MIL-53(Al)].

The above results thus clearly indicate that the observed selectivity toward the formation of DHMTHF presumably relies on the presence of free amine moieties in the frameworks of MIL-101(Al)-NH_2 and MIL-53(Al)-NH_2. Notably, recent studies also indicate that the catalysts with a nitrogen-containing support can efficiently modify their catalytic performance toward the selectivity of target product in the hydrogenation reactions.[50−52] In our case, Figure 1b illustrates the special function of the support MIL-101(Al)-NH_2 and demonstrates the step sequence for the selective hydrogenation of HMF. In the initial stage, HMF can interact with the MIL-101(Al)-NH_2 surface through hydrogen bonds to form O−H···N interactions between the hydroxyl group of the HMF and the amine group of the MIL-101(Al)-NH_2. H_2 is presumably activated by the palladium nanoparticles supported on MIL-101(Al)-NH_2. The aldehyde group of HMF is then hydrogenated to the hydroxyl group, and HMF is accordingly converted into DHMF (Figure 1b). There is, however, a stronger interaction between MIL-101(Al)-NH_2 and DHMF than that of MIL-101(Al)-NH_2 and HMF, as a result of more hydroxyl groups in the DHMF molecule and a much more hydrophilic nature of DHMF than in the case of HMF. Therefore, the in situ obtained DHMF can hardly be replaced by a fresh and more weakly binding HMF molecule, thus leading to a further hydrogenation to DHMTHF (Figure 1b).

The above assumption was further supported by adsorption experiments of HMF and DHMF over various MOFs as described in Table 2. Adsorptions of HMF or DHMF over various MOFs were investigated by addition of activated MOF to a solution of HMF or DHMF in water. The mixture was stirred, and the amounts of adsorbed HMF or DHMF over the MOFs were determined chromatographically by the corresponding concentration change of HMF or DHMF in water. In the cases of amine-functionalized MOFs, both MIL-101(Al)-NH_2 and MIL-53(Al)-NH_2 show significant adsorption of DHMF than HMF (Table 2), suggesting an enhanced interaction between DHMF and amine-functionalized MOFs through the hydrogen bonding. Moreover, the adsorption of DHMF over amine-functionalized MOFs [MIL-101(Al)-NH_2 and MIL-53(Al)-NH_2] is high than in the case of unfunctionalized MOFs [MIL-101(Cr) and MIL-53(Al)], indicating an improved hydrophilic nature both for DHMF and amine-functionalized MOFs when compared with HMF and unfunctionalized MOFs, respectively. For instance, the adsorbed DHMF over MIL-53(Al)-NH_2 and MIL-53(Al) are 1.38 and 0.33 mmol g^{-1} (Table 2), respectively, although the MIL-53(Al)-NH_2 shows dramatically low BET area of 217.6 m^2 g^{-1} when compared with the BET area of 1494.2 m^2 g^{-1} for MIL-53(Al) (Table 1). The above adsorption experiments thus indicate that the adsorptions of HMF or DHMF over various MOFs are enhanced by the hydrophilic nature of substrate

Table 2. Adsorptions of HMF and DHMF over Various MOFs

samples	HMF [mmol g^{-1}]	HMF [mmol m^{-2}]	DHMF [mmol g^{-1}]	DHMF [mmol m^{-2}]
MIL-101(Al)-NH_2	0.25	2.44×10^{-4}	0.79	7.70×10^{-4}
MIL-53(Al)-NH_2	0.22	1.01×10^{-3}	1.38	6.34×10^{-3}
MIL-53(Al)	0.56	3.75×10^{-4}	0.33	2.21×10^{-4}
MIL-101(Cr)	0.16	1.05×10^{-4}	0.37	2.44×10^{-4}

DOI: 10.1021/cs5012926
ACS Catal. 2015, 5, 722−733

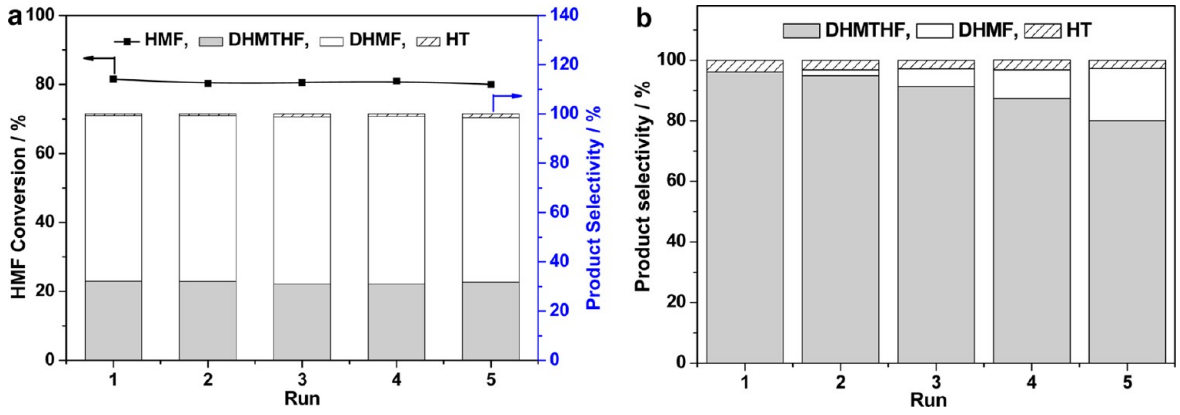

Figure 11. Reusability of Pd/MIL-101(Al)-NH_2. Reaction condition: HMF (126 mg, 1.0 mmol), Pd/MIL-101(Al)-NH_2 (20 mg, Pd 3.0 wt %), water (8 mL), H_2 (1.0 MPa), reaction temperature (30 °C), reaction time [1 h for (a) and 12 h for (b)].

molecule as well as the hydrogen bonding interactions between the substrate molecule and MOF support.

Therefore, from the point view of both metal sites and substrate molecules, the presence of an amine group in the MIL-101(Al)-NH_2 brings multifunctional advantages to the catalytic reaction system in this research. For the metal sites, the presence of amine groups on the frameworks lead to the formation of uniform and highly dispersed palladium nanoparticles over the MIL-101(Al)-NH_2 through the reaction pathway of anionic exchange and gentle reduction (Figure 1a). In the case of substrate molecules, owing to the enhanced hydrogen bonding interactions between MIL-101(Al)-NH_2 and the "intermediate" DHMF than in the case of reactant HMF, MIL-101(Al)-NH_2 promotes the further hydrogenation of DHMF to DHMTHF upon the in situ formation of DHMF under the reaction conditions, and thus improves the selectivity to the desired DHMTHF production (Figure 1b). Finally, recent research revealed that the formation of HT during the HMF hydrogenation is presumably obtained from DHMF by acid catalyzed reactions, followed by hydrogenation of ring-opening products.[12] In our case, the presence of amine group and the weak basicity of the support MIL-101(Al)-NH_2 can thus suppress the DHMF-to-HT transformation and, therefore, improve the selectivity to DHMTHF.

Catalyst Recycling. In order to probe the reusability of Pd/MIL-101(Al)-NH_2, a five-cycle experiment was performed for HMF hydrogenation at 1 h (Figure 11a) and 12 h (Figure 11b), respectively, to investigate the catalyst activity decay. Each time, the Pd/MIL-101(Al)-NH_2 was recovered by a filter, washed thoroughly with methanol–water, and then recycled for the next reaction. In the case of the recyclability tests performed at 1 h, almost identical results were observed, as shown in Figure 11a, indicating no efficiency loss for the catalyst. Under the above hydrogenation conditions, HMF conversion was low than 82% with the major hydrogenation product of DHMF (Figure 11a). Notably, a full conversion of HMF can always be achieved during the five-cycle experiments after 12 h hydrogenation of HMF (Figure 11b). However, the measured selectivity for the predominant product DHMTHF reduced from 96% to 80% (Figure 11b). The selectivity of DHMF increased from trace to 17%. Moreover, the selectivity of HT was kept around 3% during the recycling experiments. Inductively coupled plasma-atomic emission spectroscopy (ICP-AES) analysis shows that only 0.03% of the total amount of Pd had leached from Pd/MIL-101(Al)-NH_2 after the five-cycle experiment, indicating an efficient stabilization effect of the MIL-101(Al)-NH_2 support on the palladium nanoparticles (Figure 11b). However, the XRD analysis revealed that the XRD patterns of the recovered Pd/MIL-101(Al)-NH_2 show some slight variations than the fresh one (Figure 4a), indicating partial loss of crystallinity in the support MIL-101(Al)-NH_2 for the recovered catalyst after a hydrogenation time of 60 h (Figure 11b). Moreover, the BET analysis indicates that the specific surface area of Pd/MIL-101(Al)-NH_2 decreases from 615.7 $m^2\ g^{-1}$ for the fresh one to 542.8 $m^2\ g^{-1}$ for the recovered one (Figure 3 and Table 1), suggesting the adsorption of insoluble polymer generated from the reactive DHMF intermediate on the surface of the catalyst.[12] The TEM analysis of fresh Pd/MIL-101(Al)-NH_2 (Pd 3.0 wt %) reveals that highly dispersed Pd nanoparticles were well deposited on the surface of MIL-101(Al)-NH_2 with an average diameter size of 2.9 nm (Figures 5c, d). In contrast, the recovered Pd/MIL-101(Al)-NH_2 catalyst after five-time recycling (Figure 11b) had the average particle sizes of 3.3 nm (Figures 5g, h).

CONCLUSIONS

In summary, we have developed an efficient heterogeneous catalyst of palladium immobilized on amine-functionalized Metal–Organic Frameworks [Pd/MIL-101(Al)-NH_2] for selective hydrogenation of biomass-based 5-hydroxymethylfurfural (HMF) to 2,5-dihydroxymethyl-tetrahydrofuran (DHMTHF) in aqueous phase. The Pd/MIL-101(Al)-NH_2 was prepared by using a direct anionic exchange approach and subsequent gentle reduction. The presence of free amine moieties in the frameworks of MIL-101(Al)-NH_2 is suggested to play the key roles on the formation of uniform and well-dispersed palladium nanoparticles on the support. The adsorption experiments reveal that the amine-functionalized MOF supports show preferential adsorption to hydrogenation intermediate DHMF than in the case of reactant HMF, owing to an enhanced hydrophilic nature of DHMF as well as improved hydrogen bonding interactions between DHMF and the MOF support, which promotes a further hydrogenation of DHMF to DHMTHF upon the in situ formation of DHMF over Pd/MIL-101(Al)-NH_2. Moreover, our results also indicate that the observed high selectivity toward DHMTHF form HMF is closely related to the cooperation between metallic site and free amine moiety on the MOF support in the catalyst of Pd/MIL-101(Al)-NH_2. The research thus highlights new

DOI: 10.1021/cs5012926
ACS Catal. 2015, 5, 722–733

perspectives for aluminum-based and amine-functionalized MOF material for biomass transformation.

■ ASSOCIATED CONTENT

Supporting Information

The following file is available free of charge on the ACS Publications website at DOI: 10.1021/cs5012926.

Supplementary data including adsorption-desorption isotherms, XPS spectra, HMF conversion, HPLC analysis, and both GC-MS and HPLC-MS (PDF)

■ AUTHOR INFORMATION

Corresponding Author

*E-mail: chenjz@ms.giec.ac.cn. Tel./Fax: (+86)-20-3722-3380 (J.C.).

Notes

The authors declare no competing financial interest.

■ ACKNOWLEDGMENTS

We are grateful for the financial support from National Natural Science Foundation of China (21472189, 21172219, 51406211 and 21207039), National Basic Research Program of China (973 Program, 2012CB215304), 100 Talents Program of the Chinese Academy of Sciences, and Guangdong Natural Science Foundation (S2013010012986 and S2013040012615).

■ REFERENCES

(1) Tuck, C. O.; Pérez, E.; Horváth, I. T.; Sheldon, R. A.; Poliakoff, M. *Science* **2012**, *337*, 695−699.
(2) Gallezot, P. *Chem. Soc. Rev.* **2012**, *41*, 1538−1558.
(3) Chheda, J. N.; Huber, G. W.; Dumesic, J. A. *Angew. Chem., Int. Ed.* **2007**, *46*, 7164−7183.
(4) Roman-Leshkow, Y.; Chheda, J. N.; Dumesic, J. A. *Science* **2006**, *312*, 1933−1937.
(5) Huber, G. W.; Corma, A. *Angew. Chem., Int. Ed.* **2007**, *46*, 7184−7201.
(6) Huber, G. W.; Iborra, S.; Corma, A. *Chem. Rev.* **2006**, *106*, 4044−4098.
(7) van Putten, R. J.; van der Waal, J. C.; de Jong, E.; Rasrendra, C. B.; Heeres, H. J.; de Vries, J. G. *Chem. Rev.* **2013**, *113*, 1499−1597.
(8) Rosatella, A. A.; Simeonov, S. P.; Frade, R. F. M.; Afonso, C. A. M. *Green Chem.* **2011**, *13*, 754−793.
(9) Nakagawa, Y.; Tamura, M.; Tomishige, K. *ACS Catal.* **2013**, *3*, 2655−2668.
(10) Schiavo, V.; Descotes, G.; Mentech, J. *Bull. Soc. Chim. Fr.* **1991**, *128*, 704−711.
(11) Nakagawa, Y.; Tomishige, K. *Catal. Commun.* **2010**, *12*, 154−156.
(12) Alamillo, R.; Tucker, M.; Chia, M.; Pagán-Torres, Y.; Dumesic, J. A. *Green Chem.* **2012**, *14*, 1413−1419.
(13) Yang, Y. L.; Du, Z. T.; Ma, J. P.; Lu, F.; Zhang, J. J.; Xu, J. *ChemSusChem* **2014**, *7*, 1352−1356.
(14) Chen, J. Z.; Lu, F.; Zhang, J. J.; Yu, W. Q.; Wang, F.; Gao, J.; Xu, J. *ChemCatChem.* **2013**, *5*, 2822−2826.
(15) Ohyama, J.; Esaki, A.; Yamamoto, Y.; Arai, S.; Satsuma, A. *RSC Adv.* **2013**, *3*, 1033−1036.
(16) Pasini, T.; Solinas, G.; Zanotti, V.; Albonetti, S.; Cavani, F.; Vaccari, A.; Mazzanti, A.; Ranieri, S.; Mazzoni, R. *Dalton Trans.* **2014**, *43*, 10224−10234.
(17) Tucker, M. H.; Alamillo, R.; Crisci, A. J.; Gonzalez, G. M.; Scott, S. L.; Dumesic, J. A. *ACS Sustainable Chem. Eng.* **2013**, *1*, 554−560.
(18) Moreau, C.; Belgacem, M. N.; Gandini, A. *Top. Catal.* **2004**, *27*, 11−30.
(19) Buntara, T.; Noel, S.; Phua, P. H.; Melian-Cabrera, I.; de Vries, J. G.; Heeres, H. J. *Angew. Chem., Int. Ed.* **2011**, *50*, 7083−7087.
(20) Koso, S.; Ueda, N.; Shinmi, Y.; Okumura, K.; Kizuka, T.; Tomishige, K. *J. Catal.* **2009**, *267*, 89−92.
(21) Chia, M.; Pagan-Torres, Y. J.; Hibbitts, D.; Tan, Q.; Pham, H. N.; Datye, A. K.; Neurock, M.; Davis, R. J.; Dumesic, J. A. *J. Am. Chem. Soc.* **2011**, *133*, 12675−12689.
(22) Buntara, T.; Noel, S.; Phua, P. H.; Melián-Cabrera, I.; Vries, J. G.; Heeres, H. J. *Top. Catal.* **2012**, *55*, 612−619.
(23) Chen, K.; Mori, K.; Watanabe, H.; Nakagawa, Y.; Tomishige, K. *J. Catal.* **2012**, *294*, 171−183.
(24) Koso, S.; Watanabe, H.; Okumura, K.; Nakagawa, Y.; Tomishige, K. *Appl. Catal., B: Environ.* **2012**, *111−112*, 27−37.
(25) Gascon, J.; Corma, A.; Kapteijn, F.; Llabrés i Xamena, F. X. *ACS Catal.* **2014**, *4*, 361−378.
(26) Dhakshinamoorthy, A.; Opanasenko, M.; Čejka, J.; Garcia, H. *Catal. Sci. Technol.* **2013**, *3*, 2509−2540.
(27) Cohen, S. M. *Chem. Rev.* **2012**, *112*, 970−1000.
(28) Corma, A.; García, H.; Llabrés i Xamena, F. X. *Chem. Rev.* **2010**, *110*, 4606−4655.
(29) Tanabe, K. K.; Cohen, S. M. *Chem. Soc. Rev.* **2011**, *40*, 498−519.
(30) Zhao, D.; Timmons, D. J.; Yuan, D. Q.; Zhou, H.-C. *Acc. Chem. Res.* **2011**, *44*, 123−133.
(31) Farha, O. K.; Hupp, J. T. *Acc. Chem. Res.* **2010**, *43*, 1166−1175.
(32) Lee, J. Y.; Farha, O. K.; Roberts, J.; Scheidt, K. A.; Nguyen, S. T.; Hupp, J. T. *Chem. Soc. Rev.* **2009**, *38*, 1450−1459.
(33) Zhang, Y. M.; Degirmenci, V.; Li, C.; Hensen, E. J. M. *ChemSusChem* **2011**, *4*, 59−64.
(34) Akiyama, G.; Matsuda, R.; Sato, H.; Takata, M.; Kitagawa, S. *Adv. Mater.* **2011**, *23*, 3294−3297.
(35) Chen, J. Z.; Li, K. G.; Chen, L. M.; Liu, R. L.; Huang, X.; Ye, D. Q. *Green Chem.* **2014**, *16*, 2490−2499.
(36) Chen, J. Z.; Liu, R. L.; Gao, H.; Chen, L. M.; Ye, D. Q. *J. Mater. Chem. A* **2014**, *2*, 7205−7213.
(37) Chen, J. Z.; Wang, S. P.; Huang, J.; Chen, L. M.; Ma, L. L.; Huang, X. *ChemSusChem* **2013**, *6*, 1545−1555.
(38) Moon, H. R.; Lim, D.-W.; Suh, M. P. *Chem. Soc. Rev.* **2013**, *42*, 1807−1824.
(39) Dhakshinamoorthy, A.; Garcia, H. *Chem. Soc. Rev.* **2012**, *41*, 5262−5284.
(40) Hwang, Y. K.; Hong, D.-Y.; Chang, J.-S.; Jhung, S. H.; Seo, Y.-K.; Kim, J.; Vimont, A.; Daturi, M.; Serre, C.; Férey, G. *Angew. Chem., Int. Ed.* **2008**, *47*, 4144−4148.
(41) Hong, D.-Y.; Hwang, Y. K.; Serre, C.; Férey, G.; Chang, J.-S. *Adv. Funct. Mater.* **2009**, *19*, 1537−1552.
(42) Huang, Y. B.; Zheng, Z. L.; Liu, T. F.; Lü, J.; Lin, Z. J.; Li, H. F.; Cao, R. *Catal. Commun.* **2011**, *14*, 27−31.
(43) Kardanpour, R.; Tangestaninejad, S.; Mirkhani, V.; Moghadam, M.; Mohammadpoor-Baltork, I.; Khosropour, A. R.; Zadehahmadi, F. *J. Organomet. Chem.* **2014**, *761*, 127−133.
(44) Pascanu, V.; Yao, Q. X.; Gómez, A. B.; Gustafsson, M.; Yun, Y. F.; Wan, W.; Samain, L.; Zou, X. D.; Martín-Matute, B. *Chem.—Eur. J.* **2013**, *19*, 17483−17493.
(45) Huang, Y. B.; Liu, S. J.; Lin, Z. J.; Li, W. J.; Li, X. F.; Cao, R. *J. Catal.* **2012**, *292*, 111−117.
(46) Martis, M.; Mori, K.; Fujiwara, K.; Ahn, W.-S.; Yamashita, H. *J. Phys. Chem. C* **2013**, *117*, 22805−22810.
(47) Ramos-Fernandez, E. V.; Pieters, C.; van der Linden, B.; Juan-Alcañiz, J.; Serra-Crespo, P.; Verhoeven, M. W. G. M.; Niemantsverdriet, H.; Gascon, J.; Kapteijn, F. *J. Catal.* **2012**, *289*, 42−52.
(48) Guo, Z. Y.; Xiao, C. X.; Maligal-Ganesh, R. V.; Zhou, L.; Goh, T. W.; Li, X. L.; Tesfagaber, D.; Thiel, A.; Huang, W. Y. *ACS Catal.* **2014**, *4*, 1340−1348.
(49) Zhang, Y.; Thomas, A.; Antonietti, M.; Wang, X. *J. Am. Chem. Soc.* **2009**, *131*, 50−51.
(50) Wang, Y.; Yao, J.; Li, H. R.; Su, D. S.; Antonietti, M. *J. Am. Chem. Soc.* **2011**, *133*, 2362−2365.
(51) Chen, A. B.; Li, Y. L.; Chen, J. Z.; Zhao, G. Y.; Ma, L. L.; Yu, Y. F. *ChemPlusChem.* **2013**, *78*, 1370−1378.

DOI: 10.1021/cs5012926
ACS Catal. 2015, 5, 722−733

(52) Chen, J. Z.; Zhang, W.; Chen, L. M.; Ma, L. L.; Gao, H.; Wang, T. J. *ChemPlusChem.* **2013**, *78*, 142−148.
(53) Serra-Crespo, P.; Ramos-Fernandez, E. V.; Gascon, J.; Kapteijn, F. *Chem. Mater.* **2011**, *23*, 2565−2572.
(54) Couck, S.; Denayer, J. F. M.; Baron, G. V.; Rémy, T.; Gascon, J.; Kapteijn, F. *J. Am. Chem. Soc.* **2009**, *131*, 6326−6327.
(55) Gascon, J.; Aktay, U.; Hernandez-Alonso, M. D.; van Klink, G. P. M.; Kapteijn, F. *J. Catal.* **2009**, *261*, 75−87.
(56) Loiseau, T.; Serre, C.; Huguenard, C.; Fink, G.; Taulelle, F.; Henry, M.; Bataille, T.; Férey, G. *Chem.—Eur. J.* **2004**, *10*, 1373−1382.
(57) Senkovska, I.; Kaskel, S. *Microporous Mesoporous Mater.* **2008**, *112*, 108−115.
(58) Chen, G. Z.; Wu, S. J.; Liu, H. L.; Jiang, H. F.; Li, Y. W. *Green Chem.* **2013**, *15*, 230−235.
(59) Horvat, J.; Klaic, B.; Metelko, B.; Sunjic, V. *Tetrahedron Lett.* **1985**, *26*, 2111−2114.
(60) Rowsell, J. L. C.; Yaghi, O. M. *J. Am. Chem. Soc.* **2006**, *128*, 1304−1315.

DOI: 10.1021/cs5012926
ACS Catal. 2015, 5, 722−733